Commun. Comput. Phys.
doi: 10.4208/cicp.220111.281111a

Vol. **12**, No. 5, pp. 1482-1494
November 2012

Study on General Governing Equations of Computational Heat Transfer and Fluid Flow

Wang Li[1], Bo Yu[1,*], Yi Wang[1], Xin-Ran Wang[1], Qing-Yuan Wang[1] and Wen-Quan Tao[2]

[1] *Beijing Key Laboratory of Urban Oil and Gas Distribution Technology, China University of Petroleum, Beijing, 102249, People's Republic of China.*
[2] *Key Laboratory of Thermal Fluid Science and Engineering of MOE, Xi'an Jiaotong University, Xi'an, 710049, People's Republic of China.*

Received 22 January 2011; Accepted (in revised version) 28 November 2011

Communicated by Boo Cheong Khoo

Available online 22 May 2012

Abstract. The governing equations for heat transfer and fluid flow are often formulated in a general form for the simplification of discretization and programming, which has achieved great success in thermal science and engineering. Based on the analysis of the popular general form of governing equations, we found that energy conservation cannot be guaranteed when specific heat capacity is not constant, which may lead to unreliable results. A new concept of generalized density is put forward, based on which a new general form of governing equations is proposed to guarantee energy conservation. A number of calculation examples have been employed to verify validation and feasibility.

AMS subject classifications: 76M12, 80A20, 68U20

Key words: SIMPLE algorithm, general form of governing equations, conservation, generalized variable, fluid-solid coupling.

1 Introduction

A general expression for governing equations is widely used in numerical simulations of heat transfer and fluid flow, in which different variables, diffusion coefficients and source terms are written in a form of a generalized variable, a generalized diffusion coefficient and a generalized source term, respectively. There are obvious advantages by utilizing

*Corresponding author. *Email address:* lw286964103@yahoo.com.cn (W. Li), yubobox@cup.edu.cn (B. Yu), wy1031@yahoo.com.cn (Y. Wang), wangxinran719@163.com (X.-R. Wang), qingyuan19871001@126.com (Q.-Y. Wang), wqtao@mail.xjtu.edu.cn (W.-Q. Tao)

this general form, such as unified form of discretization and programming for all the governing equations, remarkable improvement on programming efficiency, enhancement of the versatility of the program as well. The popular general governing equation is written below:

$$\frac{\partial(\rho\phi)}{\partial t}+div\left(\rho U\phi\right)=div\left(\Gamma_{\phi}{}^{*}grad\phi\right)+S_{\phi}{}^{*} \tag{1.1}$$

which is a classical method widely used in many textbooks [1–8], where ϕ is a general variable to represent variables such as u, v, w and T, and $\Gamma_{\phi}{}^{*}$ is a generalized diffusion coefficient corresponding to the variable ϕ. The first and second term on the left side of Eq. (1.1) are respectively the unsteady term and the convective term, while the first term on the right side is a generalized diffusion term, and the second term $S_{\phi}{}^{*}$ is a generalized source term representing the summation of those terms in the governing equations except the unsteady term, the convective term and the diffusion term. For a two-dimensional laminar fluid flow and heat transfer in a Cartesian coordinate system, the specific meanings of $\Gamma_{\phi}{}^{*}$ and $S_{\phi}{}^{*}$ are listed in Table 1 [9, 10].

Table 1: Coefficient and source term of the popular general governing equations.

Equation	ρ	ϕ	$\Gamma_{\phi}{}^{*}$	$S_{\phi}{}^{*}$
Continuity equation	ρ	1	0	0
Momentum eqn. (x direction)	ρ	u	μ	$\rho f_x-\frac{\partial p}{\partial x}$
Momentum eqn. (y direction)	ρ	v	μ	$\rho f_y-\frac{\partial p}{\partial y}$
Energy equation	ρ	T	λ/c_p	S_T/c_p

In Table 1, x and y represent abscissa and ordinate, while u and v are the velocity components in the x- and y- coordinates; f_x and f_y are the body forces. p, ρ, μ, λ and c_p respectively indicate pressure, density, dynamic viscosity, thermal conductivity and specific heat capacity. This general expression has been widely applied in numerical heat transfer to solve a large amount of practical engineering issues. However, by the theoretical analysis in this paper, it is found that energy conservation cannot be guaranteed when specific heat capacity is not a constant, and this non-conservation may lead to unreliable results, which indicates there are some limitations of the above general form of governing equations (Eq. (1.1)). In order to ensure energy conservation, this paper puts forward a new expression of general governing equations based on theoretical analysis.

2 Analyses of proposed form of governing equations

The conservation law of a physical variable in a finite volume would only be satisfied in numerical discretization by employing conservative governing equations [4]. According to the classical heat transfer text books [11, 12], the conservative energy equation can be

expressed as follows:

$$\frac{\partial(\rho c_p T)}{\partial t}+\frac{\partial(\rho c_p u T)}{\partial x}+\frac{\partial(\rho c_p v T)}{\partial y}=\frac{\partial}{\partial x}\left(\lambda\frac{\partial T}{\partial x}\right)+\frac{\partial}{\partial y}\left(\lambda\frac{\partial T}{\partial y}\right)+S_T. \tag{2.1}$$

The above equation can be transformed to the following expression:

$$\begin{aligned}\frac{\partial(\rho T)}{\partial t}+\frac{\partial(\rho u T)}{\partial x}+\frac{\partial(\rho v T)}{\partial y}=&\frac{\partial}{\partial x}\left(\frac{\lambda}{c_p}\frac{\partial T}{\partial x}\right)+\frac{\partial}{\partial y}\left(\frac{\lambda}{c_p}\frac{\partial T}{\partial y}\right)+\frac{S_T}{c_p}\\&-\frac{1}{c_p^2}\left[\rho c_p T\frac{\partial c_p}{\partial t}+\left(\rho c_p u T-\lambda\frac{\partial T}{\partial x}\right)\frac{\partial c_p}{\partial x}+\left(\rho c_p v T-\lambda\frac{\partial T}{\partial y}\right)\frac{\partial c_p}{\partial y}\right].\end{aligned} \tag{2.2}$$

It is obvious that Eq. (2.2) is strictly equivalent to Eq. (2.1) so that Eq. (2.2) is also a conservative equation. When specific heat capacity c_p is a constant, providing $\partial c_p/\partial t=0$, $\partial c_p/\partial x=0$ and $\partial c_p/\partial y=0$, the above expression can be converted to the form below:

$$\frac{\partial(\rho T)}{\partial t}+\frac{\partial(\rho u T)}{\partial x}+\frac{\partial(\rho v T)}{\partial y}=\frac{\partial}{\partial x}\left(\frac{\lambda}{c_p}\frac{\partial T}{\partial x}\right)+\frac{\partial}{\partial y}\left(\frac{\lambda}{c_p}\frac{\partial T}{\partial y}\right)+\frac{S_T}{c_p}. \tag{2.3}$$

In this case, Eq. (2.3) is the same as Eq. (2.2). However, when c_p is not constant (i.e. $\partial c_p/\partial t\neq 0$, $\partial c_p/\partial x\neq 0$ and $\partial c_p/\partial y\neq 0$),

$$\rho c_p u T-\lambda\frac{\partial T}{\partial x}=0,\quad \rho c_p v T-\lambda\frac{\partial T}{\partial y}=0\quad\text{and}\quad \rho c_p T\frac{\partial c_p}{\partial t}=0 \tag{2.4}$$

should be satisfied simultaneously to guarantee the equivalence between Eq. (2.2) and Eq. (2.3) if Eq. (2.3) is still considered the same as Eq. (2.2) strictly. Obviously, these three expressions cannot always be met so that Eq. (2.3) is a non-conservative equation and not strictly equivalent to Eq. (2.2). The lacking term

$$-\frac{1}{c_p^2}\left[\rho c_p T\frac{\partial c_p}{\partial t}+\left(\rho c_p u T-\lambda\frac{\partial T}{\partial x}\right)\frac{\partial c_p}{\partial x}+\left(\rho c_p v T-\lambda\frac{\partial T}{\partial y}\right)\frac{\partial c_p}{\partial y}\right] \tag{2.5}$$

can cause the results by Eq. (2.3) are quite different from those by Eq. (2.2), especially for problems with dramatic varying c_p which are often encountered in engineering applications. For example, the specific heat capacity of heated crude oil during the transportation or shutdown process may vary dramatically with temperature. Another example is a fluid-solid coupling problem, which the specific heat capacity jumps suddenly at the interface of fluid and solid. For these problems, the application of Eq. (2.3) may lead to inaccurate or distortive results which mean that it is no longer applicable to this kind of engineering simulations. Therefore, Eq. (2.3) should be used cautiously when c_p is not constant. However, the non-conservative equation (Eq. (2.3)) has been widely used even if the specific heat capacity is not constant. The survey of all the papers published in 2010 in International Journal of Heat and Mass Transfer reveals that totally 163 papers

used conservative energy equations, among which 71 papers (about 44%) adopted the format of Eq. (2.3). This is a big amount, and it is similar for other journals. Therefore, it is absolutely necessary to study the differences between the two expressions of energy equation, i.e. Eq. (2.1) (or Eq. (2.2)) and Eq. (2.3).

To deal with these problems, energy conservation at any c_p, whether constant or not, should be ensured. For such a purpose, we propose a new expression below:

$$\frac{\partial(\rho^*\phi)}{\partial t}+div\left(\rho^* U\phi\right)=div\left(\Gamma_\phi grad\phi\right)+{S_\phi}^*, \tag{2.6}$$

where ρ^*, Γ_ϕ and ${S_\phi}^*$ represent respectively generalized density, which is different from the one used in Eq. (1.1), actual diffusion coefficient and generalized source term. The three terms are shown in Table 2 for a two-dimensional system.

Table 2: Coefficient and source term of the newly proposed general governing equations.

Equation	ρ^*	ϕ	Γ_ϕ	${S_\phi}^*$
Continuity equation	ρ	1	0	0
Momentum eqn. (x direction)	ρ	u	μ	$\rho f_x-\frac{\partial p}{\partial x}$
Momentum eqn. (y direction)	ρ	v	μ	$\rho f_y-\frac{\partial p}{\partial y}$
Energy equation	ρc_p	T	λ	S_T

Comparing Eq. (2.6) with Eq. (1.1) and Table 2 with Table 1, we can see that the new general form has two advantages: energy conservation is ensured and Γ_ϕ is always the actual diffusion coefficient. Based on the new form, two computational examples are presented to analyze the difference between these two kinds of general forms of governing equations on the following aspects: 1) mixed convection, 2) fluid-solid coupling heat transfer.

3 Computational results and discussion

Based on SIMPLE algorithm with staggered grid, QUICK scheme and central difference scheme are employed in discretization of convective term and diffusion term, respectively. Non-uniform grid of 80×80 is used for mixed convection while uniform grid of 80×80 is adopted for fluid-solid coupling problem. Before the comparison study, we have validated our numerical code by test calculations for lid-driven and square cavity natural convection problems and good agreements have been obtained between our solutions and benchmark solutions [13–15]. We also validated our numerical code very well through other works using mixed convection problems [16–18]. Thus, our numerical procedure is reliable. In all the calculations below, the numerical results are independent of meshes. For quantitative comparison of the two general expressions of governing equations, a relative deviation E of the Nusselt number is defined as $E=|Nu-Nu^*|/Nu^*\times$

100%, where Nu and Nu^* represent Nusselt number obtained by Eq. (1.1) and Eq. (2.6), respectively. In order to observe the differences between the two general governing equations when c_p is not a constant, the flow media with temperature-varying behavior and space-jumping behavior of c_p are chosen for the two problems in Sections 3.1 and 3.2 respectively.

3.1 Numerical results of mixed convection

The numerical example of a mixed convection in a closed square cavity with the side length $L=0.025$m is shown in Fig. 1. The bottom and top temperatures are 50°C and -10°C, respectively. Both the left and the right walls are adiabatic. Non-slip boundary condition is employed for all walls. The lid velocity is 0.2m/s. Physical properties of the fluid are: $\rho=1000\text{kg/m}^3$, $\mu=5.0\times10^{-3}$Pa·s, $\lambda=0.5\text{W/(m·°C)}$, $\beta=1.0\times10^{-4}\text{K}^{-1}$ (correlate with Grashof number, see details in Nomenclature), $c_p=0.0011T^4-0.09T^3+0.09T^2+111T+1993$(J/kg·°C). The variation of c_p with temperature is shown in Fig. 2. According to these properties, Reynolds number Re and Grashof number Gr can be calculated as 1000 and 36750 respectively. The results obtained from Eq. (2.6) are compared with those from Eq. (1.1) to explain the necessity of Eq. (2.6), and then the computational speeds of these two methods are compared to test the grid sensitivity.

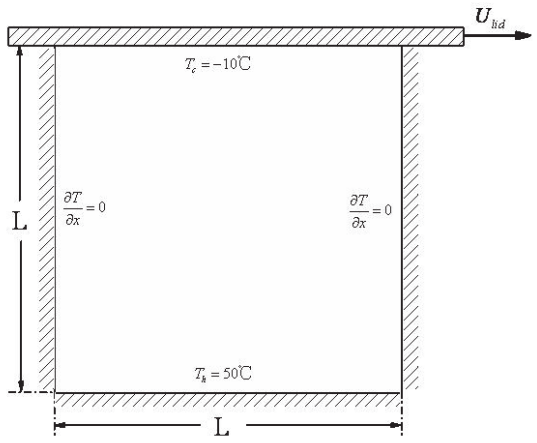

Figure 1: Computational domain of mixed convection.

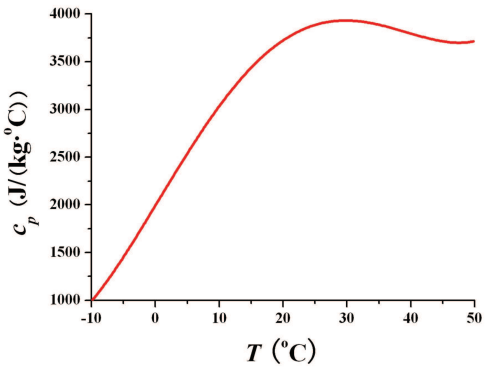

Figure 2: Specific heat capacity vs. temperature.

The temperature field and corresponding specific heat capacity distribution obtained by employing Eq. (2.6) are shown in Fig. 3. It is apparent to see that, from Fig. 3(a), c_p has large variation in the temperature range -10°C$\sim$50°C (from about 1300 to about 3750 in Fig. 2). Larger c_p mainly appears in the lower corners while in most of the region c_p has smaller values. When we use Eq. (1.1) in the calculation, c_p needs to be assumed as a constant, which deviates the real situation greatly, making Eq. (1.1) can hardly capture the accurate features of the real field. To quantitatively show this, we did calculations by

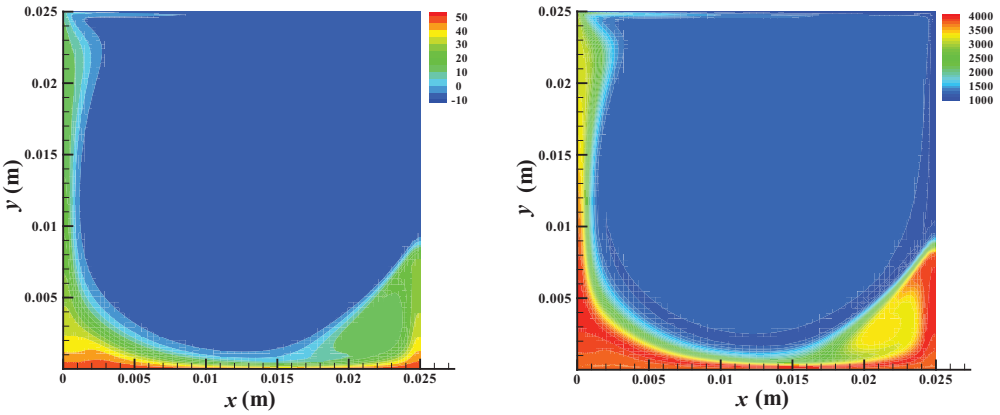

(a) Temperature distribution (b) Specific heat capacity distribution

Figure 3: Field results obtained by Eq. (2.6).

using Eq. (1.1) with five commonly used average formulations of c_p, i.e.,

1. arithmetic mean of the values at the extreme temperatures, $c_1=(c_{p_{T_h}}+c_{p_{T_c}})/2$;
2. evaluated the expression of c_p by arithmetic mean temperature of the extreme ones, $c_2=c_p((T_h+T_c)/2)$;
3. weighted average, $c_3=\int_{T_c}^{T_h}c_p dT/\int_{T_c}^{T_h}dT$;
4. evaluated by the mean fluid temperature, $c_4=c_p(\int_0^L\int_0^L T dxdy/\int_0^L\int_0^L dxdy)$;
5. area weighted average, $c_5=\int_0^L\int_0^L c_p dxdy/\int_0^L\int_0^L dxdy$.

Fig. 4(a) compares Nusselt numbers obtained by Eq. (1.1) with that by Eq. (2.6) using the above five average methods. It can be seen that Nusselt numbers along the horizontal wall predicted by the five average c_p deviate from the correct one (Nu obtained by Eq. (2.6)) apparently. Analyzing the relative deviations caused by these five methods in details, as shown in Fig. 4(b), we can clearly find that the overall relative deviations between Eq. (1.1) and Eq. (2.6) are very large with the maximum deviation on the right side (24.5%) at $X=0.95$ for c_5 and the maximum deviation on the left side (16.6%) at $X=0.13$ for c_2 ($X=x/L$). The maximum deviations for all the five average formulations appear in the regions $X=0\sim0.2$ and $X=0.8\sim1.0$. This is because the real c_p is much larger in these regions (Fig. 3(b)) and average c_p has larger difference from the real values. In a word, the application of Eq. (1.1) cannot obtain accurate enough results, no matter which average c_p is assumed. Moreover, these differences will not be changed with increasing grid numbers since the results are all grid independent. Therefore, the differences between Eq. (2.6) and Eq. (1.1) are due to the different expressions of themselves, but not grid numbers as well as the functional forms of c_p.

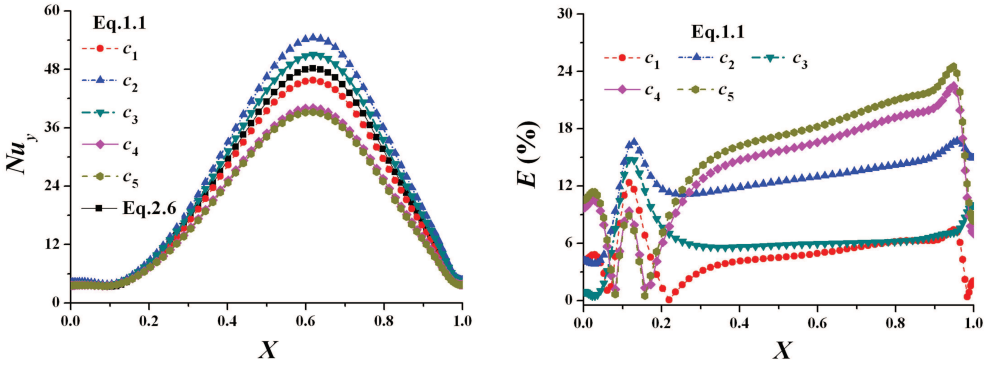

(a) Nusselt number (b) Relative deviation

Figure 4: Comparison of Nusselt number and relative deviation of mixed convection at grid number 80×80.

Another important issue is to compare the computational speed of the new method with that of the classical method using different grid numbers. Additional 4 sets of grids are employed, i.e. 20×20, 40×40, 60×60 and 100×100. The computational time of the new method and the classical method with the five average methods are compared in Fig. 5. The computational speed differences among different mean methods of c_p in Eq. (1.1) are due to different Prandtl numbers ($Pr=v/a=\mu c_p/\lambda$) resulting from the different c_p values since other parameters are constant (Table 3). It is well known that the larger Prandtl number leads to larger computational time in the simulation of heat transfer problems. From Fig. 5, the c_p values have the sequence that $c_2>c_3>c_1>c_5>c_4$. Accordingly, the computational time also has the sequence that $t_2>t_3>t_1>t_5>t_4$. It is clear that the larger c_p is, the slower the computation will be. The reason can be found in Fig. 2 and Fig. 3 that c_p is small in most of the region so that the actual mean c_p is closer to small value. Thus, the average method which can obtain smaller mean c_p is closer to the real situation and

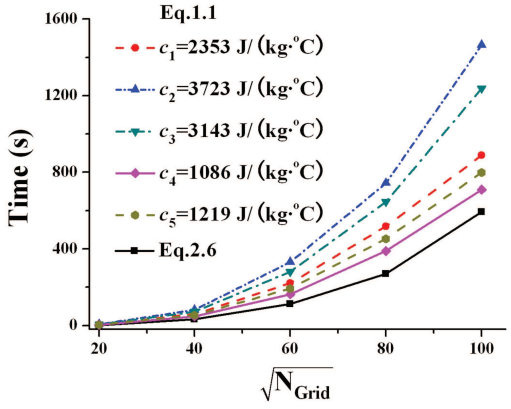

Figure 5: Computational time for different grid numbers.

Table 3: Prandtl number and specific heat capacity for different average methods.

	c_1	c_2	c_3	c_4	c_5
c_p (J/(kg·°C))	2354	3723	3143	1086	1219
μ (Pa·s)	0.005	0.005	0.005	0.005	0.005
λ_f (W/(m·°C))	0.5	0.5	0.5	0.5	0.5
Pr	23.54	37.23	31.43	10.86	12.19

has smaller computational time. Computational time of Eq. (2.6) is smaller and smaller than those of Eq. (1.1) with increasing grid number. Take the grid number 100×100 as an example, the highest and lowest computational time using Eq. (1.1) are 1465s and 709s respectively while the computational time using Eq. (2.6) is only 593s. That is to say the computational time of the classical method is as much as $1.2\sim2.5$ times of that of newly proposed one. It should be noted here that the small computational time of Eq. (2.6) in this case is due to the small Pr (i.e. small c_p) in most of the region. For the case that Pr is large in most of the region, computation using Eq. (2.6) may be slower than that using Eq. (1.1).

In a word, Eq. (1.1) cannot reflect the real features of heat transfer in this case due to its non-conservative quality. Therefore, it should not be applied to this kind of problems. Instead, Eq. (2.6) should be used since it can maintain energy conservation.

3.2 Numerical results of fluid-solid coupling heat transfer

The above example illustrates that computational results of the popular general governing equations can hardly satisfy the needs of actual projects due to non-conservative energy equation, which is caused by considerable change of specific heat capacity c_p with temperature. On the other hand, as to the fluid-solid coupling heat transfer solved by full-field computation methods, even if the variation of specific heat capacity c_p with temperature for each part of fluid and solid could be neglected, jump (sudden change) of c_p in the computational domain caused by different physical properties of fluid and solid may lead to distorted or even erroneous results when using the popular general governing equations. When Eq. (1.1) is used in the computation, at the fluid-solid interface the expression

$$\frac{\lambda_f}{c_{p_f}}\left(\frac{\partial T}{\partial y}\right)_f=\frac{\lambda_s}{c_{p_s}}\left(\frac{\partial T}{\partial y}\right)_s \tag{3.1}$$

is to be satisfied. The unequal specific heat capacity of fluid and solid, $c_{p_f}\neq c_{p_s}$ gives rise to disparate heat flux

$$\lambda_f\left(\frac{\partial T}{\partial y}\right)_f\neq\lambda_s\left(\frac{\partial T}{\partial y}\right)_s. \tag{3.2}$$

This is, however, inconsistent with actual physical process, leading to erroneous result. Obviously, the greater difference of c_p between fluid and solid, the more distorted calculation result. To ensure the continuity of the flux rate at the interface, Han and Chen [19]

put forward a solution: the thermal conductivity of fluid adopts individual value, while the heat capacity of the solid takes the value of the fluid. This method has been used in [4, 20]. However,

$$\lambda_f\left(\frac{\partial T}{\partial y}\right)_f=\lambda_s\left(\frac{\partial T}{\partial y}\right)_s \tag{3.3}$$

is the default condition of the newly proposed general governing equation on the fluid-solid coupling boundary, and is consistent with actual physical process. Apparently, the new method is much easier to be implemented than that proposed by Han and Chen dealing with complicated fluid-solid coupling issues.

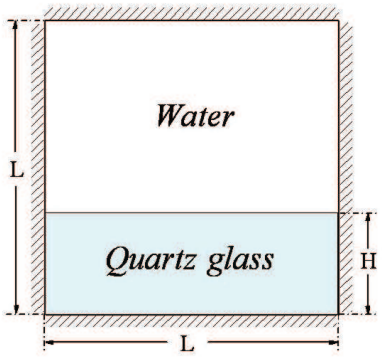

Figure 6: Region distribution diagram for a fluid-solid coupling problem.

Take the fluid-solid coupling case shown in Fig. 6 as an example. Water and quartz glass are chosen as the computation media, whose physical properties are shown in Table 4. The size of computational domain is $L\times L=0.01\text{m}\times 0.01\text{m}$ and two heights of solid region are considered: $H=0.002\text{m}$ (case 1), $H=0.004\text{m}$ (case 2). All the walls of the computational domain are stationary. The left and the right walls are maintained 70°C and 10°C respectively, and the other two walls are thermal insulated.

Table 4: Physical properties of water and quartz glass.

	Density ρ (kg/m^3)	Heat capacity c_p (J/K)	Heat conductivity λ (W/(m·K))	Dynamic viscosity μ (Pa·s)	Thermal expansion coefficient β (1/K)
Water	998.23	4181.8	0.5984	1.002×10^{-3}	6.9×10^{-5}
Quartz glass	2180	750	1.38	$+\infty$	—

Solving the example described above by the popular general governing Eq. (1.1) and the newly proposed general governing Eq. (2.6), we could generate isotherms as in Fig. 7, which shows remarkable discrepancy. Fig. 8(a) shows the Nusselt number curve at the left side of computational domain while Fig. 8(b) shows the relative deviation E, from which it can be observed that the maximum and average deviations of Nusselt number

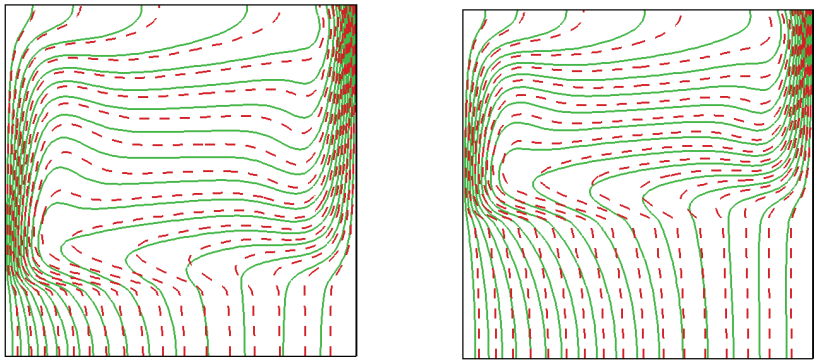

(a) case 1, $H=0.002$m (b) case 2, $H=0.004$m

Figure 7: Isotherms of fluid-solid coupling.

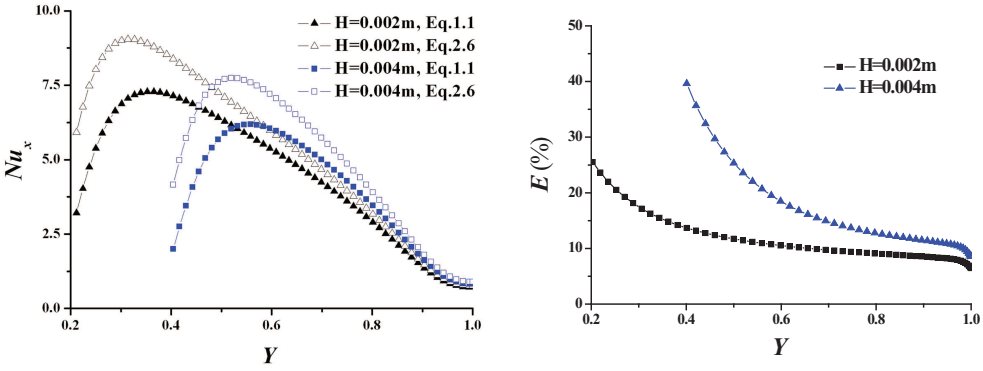

(a) Nusselt number (b) Relative deviation

Figure 8: Comparison of Nusselt number and relative deviation of fluid-solid coupling heat transfer.

are 56.59% and 20.23% respectively for case 1, while those are 55.33% and 23.01% for case 2. The large E is due to a large jump (sudden change) of specific heat capacity at the interface, from in the water region to in the solid region. Apparently, the newly proposed general governing Eq. (2.6) should be applied when the jump of specific heat capacity at the fluid-liquid interface is encountered.

The condition satisfied at the fluid-solid coupling boundary, given by Eq. (1.1), is

$$\frac{0.5984}{4181.8}\left(\frac{\partial T}{\partial y}\right)_f=\frac{1.38}{750}\left(\frac{\partial T}{\partial y}\right)_s \quad \text{or} \quad \frac{(\partial T/\partial y)_f}{(\partial T/\partial y)_s}=12.86, \tag{3.4}$$

having a serious deviation from the following equality condition of heat flux by Eq. (2.6):

$$0.5984\left(\frac{\partial T}{\partial y}\right)_f=1.38\left(\frac{\partial T}{\partial y}\right)_s \quad \text{or} \quad \frac{(\partial T/\partial y)_f}{(\partial T/\partial y)_s}=2.3. \tag{3.5}$$

This is the fundamental reason for the variation.

All the cases mentioned above are laminar convective heat transfer, however, conservative governing equations could be also recommended for turbulent convective heat transfer and mass diffusion. Table 5 shows the recommended expressions for ρ^*, ϕ, $\Gamma_\phi{}^*$ and $S_\phi{}^*$, in which, c_s, ρc_s, D_s, μ_T and Pr_T respectively represent volume concentration of component s, mass concentration, diffusion coefficient of component s, turbulent viscosity and turbulent Prandtl number.

Table 5: Coefficients and source term of governing equations for turbulent convective heat transfer and component diffusion.

	Equation	ρ^*	ϕ	Γ_ϕ	$S_\phi{}^*$
Traditional general governing equation	Component mass conservation equation	ρ	c_s	ρD_s	S_s
	Turbulent energy equation	ρ	T	$\frac{\mu}{Pr}+\frac{\mu_T}{Pr_T}$	$\frac{S_T}{c_p}$
Proposed general governing equations	Component mass conservation equation	1	ρc_s	D_s	S_s
	Turbulent energy equation	ρc_p	T	$c_p(\frac{\mu}{Pr}+\frac{\mu_T}{Pr_T})$	S_T

4 Conclusions

This paper analyzes the general governing equations commonly used in computational heat transfer and fluid flow and points out the limitations. Energy conservation of the popular general governing equations cannot be guaranteed when specific heat capacity varies with temperature or changes in space. The commonly used equations may result in distorted or even erroneous results no matter which average method for heat capacity is used. Based on theoretical analysis, the new general governing equations have been proposed, using generalized density and generalized source term to distinguish different physical equations. Conservation of all these expressions has been proved well by computational examples.

Acknowledgments

The study is supported by the National Natural Science Foundation of China (No. 51176204 and No. 51134006), and the State Key Laboratory of Multiphase Flow in Power Engineering (Xi'an Jiaotong University). We appreciate Dr. Hiroyuki Ozoe, Professor Emeritus of Kyushu University, Japan, on his comments in preparing the revised version of this paper. The helpful comments of reviewers are greatly appreciated.

Nomenclature

a thermal diffusivity (m^2/s), $a=\frac{\lambda}{\rho c_p}$

c_p specific heat capacity under constant pressure (J/(kg·°C))

c_1 arithmetic mean of c_p at the extreme temperatures (J/(kg·°C)), $c_1=(c_{p_{T_h}}+c_{p_{T_c}})/2$

c_2 c_p evaluated by mean temperature of the extreme ones (J/(kg·°C)), $c_2=c_p((T_h+T_c)/2)$

c_3 weighted average of c_p (J/(kg·°C)), $c_3=\int_{T_c}^{T_h}c_p dT/\int_{T_c}^{T_h}dT$

c_4 c_p evaluated by the weighted mean temperature (J/(kg·°C)), $c_4=c_p(\int_0^L\int_0^L T dxdy/\int_0^L\int_0^L dxdy)$

c_5 area weighted average of c_p (J/(kg·°C)), $c_5=\int_0^L\int_0^L c_p dxdy/\int_0^L\int_0^L dxdy$

c_s volume concentration of component s; D_s diffusion coefficient

f_x body force in the x- coordinate (m/s^2); f_y body force in the y- coordinate (m/s^2)

Gr Grashof number, $Gr=\rho^2\beta g(T_h-T_c)L^3/\mu^2$

L side length of the square cavity (m)

Nu_x Nusselt number on the vertical walls, Nu_x=$\partial\theta/\partial X$

Nu_y Nusselt number on the horizontal walls, Nu_y=$\partial\theta/\partial Y$

$\overline{Nu}$ average Nusselt number

Pr Prandtl number, $Pr=v/a$; Pr_T turbulent Prandtl number

p pressure (Pa); Re Reynolds number, $Re=\rho uL/\mu$

$S_\phi{}^*$ generalized source term; S_T heat source (W/m^3)

T temperature of computation media (°C)

T_h temperature of the hot wall (°C); T_c temperature of the cold wall (°C)

t time (s); t_i computational time by using Eq. (1.1) with c_i (s), $1\le i\le 5$

u velocity component in the x-coordinate (m/s)

v velocity component in the y-coordinate (m/s)

x horizontal direction (m); y vertical direction (m)

X non-dimensional abscissa, $X=x/L$; Y non-dimensional ordinate, $Y=y/L$

Greek symbols

β thermal expansion coefficient (1/K) $\Gamma_\phi{}^*$ generalized diffusion coefficient

θ non-dimensional temperature, $\theta=T/(T_h-T_c)$

λ thermal conductivity (W/(m·°C)) μ dynamic viscosity (Pa·s)

μ_T turbulent viscosity (Pa·s) v kinetic viscosity (m^2/s)

ρ density (kg/m^3) ρ^* generalized density

ϕ general variable to represent u, v, w, T etc.

References

[1] S.V. Pantanker, Numerical Heat Transfer and Fluid Flow, Hemisphere Publishing Corporation,1980.
[2] H.K. Versteeg, W. Malalsekera, An Introduction to Computational Fluid Dynamics, The Finite Volume Method. Essex: Longman Scientific and Technical, 1995.
[3] P. Wesseling, Principles of Computational Fluid Dynamics, Science Press, Beijing, 2001
[4] W.Q. Tao, Numerical Heat Transfer, 2nd ed., Xi'an Jiaotong University Press, Xi'anA2002.
[5] J.H. Ferziger, M. Peric, Computational Methods for Fluid Dynamics, Springer, 2002.
[6] A.W. Date, Introduction to Computational Fluid Dynamics, Cambridge: Cambridge University Press, 2005
[7] R.W. Lewis, P. Nithiarasu, K.N. Seetharamu, Fundamentals of the Finite Element Method for Heat and Fluid Flow, John Wiley & Sons,Ltd, 2008
[8] W.J. Minkowycz, E.M. Sparrow, J.Y.J. Murthy, Handbook of Numerical Heat Transfer, Second Edition, John Wiley & Sons, Ltd, 2009
[9] T.Y. Long, Y.X. Su, W.Y. Xiang, C. He, Computational Fluid Dynamics, Chongqing, Chongqing University Press, 2007.
[10] S.V. Pantanker, Recent developments in computational heat transfer, J. Heat Transfer, Vol. 110, No. 4, pp. 1037-1046, 1988.
[11] R.B. Bird, W.E. Stewart, E.N. Lightfoot, Transport Phenomena, John Wiley & Sons, Inc, 2002.
[12] J.P. Holman, Heat Transfer, McGraw-Hill, New York, 2002.
[13] G. Barakos, E. Mitsoulis, D. Assimacopoulos, Natural convection flow in a square cavity, Int. J. Numer. Methods Fluids, Vol. 18, pp. 695-719, 1994.
[14] O. Botella, R. Peyret. Benchmark spectral results on the lid-driven cavity flow, Comput. Fluids, Vol. 27, No. 4, pp. 421-433, 1998.
[15] C.H. Bruneau, M. Saad, The 2D lid-driven cavity problem revisited, Comput. Fluids, Vol. 35, pp. 326-348, 2006.
[16] O. Aydin, Aiding and opposing mechanisms of mixed convection in a shear and buoyancy-driven cavity, Int. Commun. Heat Mass Transfer, Vol. 26, pp. 1019-1028, 1999.
[17] H.F. Oztop, I. Dagtekin, Mixed convection in two-sided lid-driven differentially heated square cavity, Int. J. Heat Mass Transfer, Vol. 47, pp. 1761-1769, 2004.
[18] N. Alleborn, H. Raszillier, F. Durst, Lid-driven cavity with heat and mass transport, Int. J. Heat Mass Transfer, Vol. 42, pp. 833-853, 1999.
[19] P. Han, X. Chen, Discussion on integral solution method for solid-liquid interaction problems, Proceedings of 7th National Symposium on Computational Heat Transfer, Beijing, pp. 32-37,1997.
[20] Z.G. Qu, W.Q. Tao, Y.L. He, Three dimensional numerical simulation on laminar heat transfer and fluid flow characteristics of strip fin surfaces with X-arrangement of strips, J. Heat Transfer, Vol. 126, No. 4, pp. 697- 707, 2004.